See related commentary on pg 529

Akt1 Controls Insulin-Driven VEGF Biosynthesis from Keratinocytes: Implications for Normal and Diabetes-Impaired Skin Repair in Mice

Itamar Goren[1,3], Elke Müller[1,3], Dana Schiefelbein[1], Paul Gutwein[1], Oliver Seitz[2], Josef Pfeilschifter[1] and Stefan Frank[1]

Here we investigated the potential role of protein kinase B (Akt) in normal or diabetes-impaired wound healing in mice. Interestingly, Akt1 was predominant in skin, wound tissue, and human keratinocytes cell line. Acute skin repair was characterized by an increase of Akt1 phosphorylation in wound margin keratinocytes. By contrast, phosphorylated Akt1 was nearly completely absent and paralleled by a poor phosphorylation of the eucaryotic initiation factor 4E-binding protein 1 (4E-BP1) and reduced levels of vascular endothelial growth factor (VEGF) protein in chronic wounds of diabetic *ob/ob* mice. Inhibition of the phosphatidyl-inositol-3 kinase/Akt pathway by wortmannin and specific abrogation of Akt1 protein using small-interfering RNA revealed a regulatory function of Akt1 in insulin-mediated VEGF biosynthesis in keratinocytes. Insulin-induced VEGF protein biosynthesis in keratinocytes was mediated by Akt1 from a constitutive VEGF-encoding mRNA pool at the posttranscriptional level through a downstream phosphorylation 4E-BP1. Moreover, transfection experiments introducing a constitutively active mutant of Akt1 into keratinocytes revealed the mammalian target of rapamycin kinase as a downstream mediator of Akt1-linked 4E-BP1 phosphorylation and translational control. Our data suggest that the endocrine hormone insulin contributes to VEGF release in skin wounds through an Akt1-mediated posttranscriptional mechanism in keratinocytes.

Journal of Investigative Dermatology (2009) **129,** 752–764; doi:10.1038/jid.2008.230; published online 31 July 2008

INTRODUCTION

Wound healing of the skin represents the highly coordinated response of an organism to deal with external injuries (Martin, 1997; Singer and Clark, 1999). However, there are a number of well-described pathological conditions that severely interfere with a successful wound closure. Among those, the diabetic foot ulcer represents a serious wound healing complication that is characterized by a loss of epithelium and dermis that may sometimes also involve muscle and bone (Reiber and Ledoux, 2002; Boulton, 2004). Unfortunately, foot ulcers of both types of diabetes mellitus are associated with a significant mortality (Carrington *et al.*, 2001; Reiber and Ledoux, 2002). Diabetic ulcers still have a poor prognosis with assessed 3-year survival rates of only about 50% in developed European countries (Apelqvist *et al.*, 1993; Faglia *et al.*, 2001).

Obviously, diabetes-disturbed wound healing must be functionally connected to prolonged and exacerbated inflammatory conditions in genetically diabetic mice (Wetzler *et al.*, 2000; Goren *et al.*, 2003, 2006) and also in man (Loots *et al.*, 1998). Interestingly, resolution of exacerbated inflammatory conditions in wound tissue from *ob/ob* mice by recombinant leptin or antibody-mediated inactivation of wound macrophages (Goren *et al.*, 2006, 2007) demonstrated that a severe insulin resistance of resident wound cells contributes to disturbed tissue movements in chronic wounds of diabetic mice. Moreover, these findings strongly suggest that insulin, beside its well-known glucose-controlling endocrine functions, participates in tissue repair by activation of the insulin signaling pathway in wound tissue (Goren *et al.*, 2006). This notion is further supported by findings that report a function of insulin and insulin-like growth factor 1 in the expressional control of the angiogenetic factor vascular endothelial growth factor (VEGF) via activation of the phosphatidylinositol 3-kinase (PI3K)/protein kinase B (Akt) in diverse cell types including epithelial cells (Treins *et al.*, 2002; Jiang *et al.*, 2003; Poulaki *et al.*, 2003; He *et al.*, 2006).

To date, only little is known about a potential role of insulin itself in diabetes-impaired wound tissue and also

[1]*Pharmazentrum Frankfurt/ZAFES, Frankfurt am Main, Germany and* [2]*Klinik für Mund-, Kiefer und Plastische Gesichtschirurgie, Klinikum der Johann Wolfgang Goethe-Universität, Frankfurt am Main, Germany*

[3]*These authors contributed equally to this study*

Correspondence: Dr Stefan Frank, Pharmazentrum Frankfurt, Institut für Allgemeine Pharmakologie und Toxikologie, Klinikum der JW Goethe-Universität Frankfurt/M., Theodor-Stern-Kai 7, D-60590 Frankfurt/M., Germany. E-mail: s.frank@em.uni-frankfurt.de

Abbreviations: Akt, protein kinase B; 4E-BP1, eucaryotic initiation factor 4E-binding protein; EGF, epidermal growth factor; GSK, glycogen synthase kinase; HaCaT, human keratinocyte cell line; mTOR, mammalian target of rapamycin; PI3K, phosphatidyl-inositol-3 kinase; siRNA, small-interfering RNA; VEGF, vascular endothelial growth factor

Received 14 December 2007; revised 24 April 2008; accepted 5 May 2008; published online 31 July 2008

intracellular signaling processes that drive and integrate insulin, cytokine- or growth factor-mediated cellular decisions at the wound site. One key molecule of the insulin signaling pathway at the crossroads from activated cytokine and growth factor receptors is Akt (Plas and Thompson, 2005), representing three highly conserved isoforms: Akt1, Akt2, and Akt3 (Testa and Tsichlis, 2005) and a target of active PI3K (Franke *et al.*, 1995). The subsequent enzymatic activation of Akt is mediated by phosphatidylinositol-dependent kinase (PDK)-1 and the mammalian target of rapamycin (mTOR)/rapamycin-insensitive companion of mTOR through phosphorylation of Akt in its activation loop (Thr308) and C-terminal tail (Ser473), respectively (Sarbassov *et al.*, 2005).

Here, we determined Akt1 to represent the predominant isoform in murine wound healing and in the human keratinocyte cell line (HaCaT). Phosphorylated Akt1 was present in wound margin keratinocytes during acute skin repair, but appeared markedly reduced in diabetes-impaired wound tissue. We observed that only insulin-, but not cytokine or growth factor-induced VEGF production was restrictively dependent on Akt activation in keratinocytes.

RESULTS

Akt expression and phosphorylation in skin and wound tissue of healthy and insulin-resistant diabetic *ob/ob* mice

First, we investigated the expression and phosphorylation of the Akt 1–3 isoforms during acute and diabetes-disturbed skin repair in diabetic *ob/ob* mice. We observed a moderate increase of mRNAs encoding Akt1 and Akt3 during the inflammatory phase of normal repair (Figure 1a). All three Akt isoforms were present at the protein level in acute healing, with particularly low levels of Akt3 in immunoblot analyses (Figure 1b, see also Figure 4c). However, we observed a marked increase in total Akt phosphorylation at residues Ser473 and Thr308 during repair, which is described to be pivotal for Akt enzymatic activation (Sarbassov *et al.*, 2005). Akt phosphorylation was paralleled by a subsequent phosphorylation of glycogen synthase kinase (GSK)-3α/β (Ser21/9; Figure 1b) and eucaryotic initiation factor 4E-binding protein 1 (4E-BP1; Figure 5c) that are both described to represent targets for Akt enzymatic activity (Cross *et al.*, 1995; Segrelles *et al.*, 2004). By contrast, disturbed wound tissue of diabetic *ob/ob* mice was characterized by reduced levels of Akt1 and a nearly complete absence of Akt2 and Akt3 protein compared to healing conditions in healthy animals (Figure 2b, left panels). By contrast, wound tissue mRNA pools for Akt1 were not reduced in diabetic *ob/ob* mice (Figure 2a), indicating that the observed loss of Akt1 protein (Figure 2b) was not a consequence of impaired Akt1 mRNA synthesis. Moreover, the marked phosphorylation of Akt at either Thr308 or Ser473 residues as well as the subsequent phosphorylation of GSK-3α/β was absent in wound tissue of diabetic *ob/ob* mice (Figure 2b, right panels). The absence of a marked phosphorylation of Akt in diabetes-impaired wound tissue was confirmed by direct quantification of phosphorylated Akt by enzyme-linked immunosorbent assay at day 5 (Figure 2c, left panel) and by immunoblot analyses at day 13

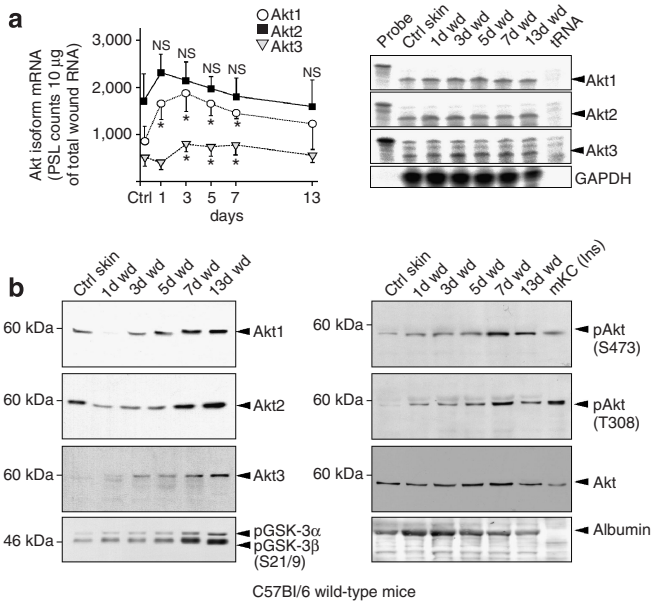

Figure 1. Expression and phosphorylation of Akt in normal skin repair. Regulation of Akt isoform mRNA (**a**) and protein (**b**) expression (left panels) or phosphorylation (right panels) in C57BL/6 mice as assessed using the RNase protection assay or immunoblot. The time after injury is indicated at the top of each lane. Ctrl skin refers to back skin biopsies of nonwounded mice. 1,000 c.p.m. of the hybridization probe were added to the lane-labeled probe. Hybridization against GAPDH was used as a loading control. A lysate of insulin-stimulated murine primary keratinocytes (mKC, Ins) was used to provide specificity of anti-Akt antibodies. A quantification of Akt1, Akt2, and Akt3 mRNA (PhosphoImager PSL counts per 10 µg of total wound RNA) is shown in the left panel. *, $P<0.05$; NS, not significant (ANOVA, Dunnett's method) as compared to control skin. Bars indicate the mean ± SD obtained from wounds ($n=48$) isolated from animals ($n=12$) from three independent animal experiments. For immunoblot analysis, each time point depicts eight wounds ($n=8$) from four individual mice ($n=4$). One representative blot from three independent experimental animal series is shown. Loading of immunoblots was controlled using a total Akt or Ponceau S staining as indicated. d, days.

post-wounding (Figure 2c, right panel). Here, it is important to note that the reduction in phosphorylated Akt in wound tissue appeared to depend at least partially on the availability of total Akt protein also, which was reduced in 5- and 13-day wounds of *ob/ob* mice (Figure 2c).

Using immunohistochemistry, we determined the localization of activated Akt during acute skin repair. Keratinocytes located at the margins of the wound exhibited particularly strong signals for phosphorylated Akt (Ser473, Thr308) and GSK-3α/β (Ser21/9; Figure 3). A histology to control specificity of the phosphorylated Akt antibodies is shown in Figure S1.

As a next step, we separated 5-day wound tissue of normal mice into wound margin (enriched for the proliferative wound margin keratinocytes) and inner wound (including the granulation tissue) sections (Figure 4a, left panel) and nonwounded tail skin into epidermis and dermis (Figure 4a, right panel) to allow a more detailed analysis. Epidermal–dermal separation was controlled using loricrin as a specific keratinocyte expression marker (Figure 4a, right panel). The

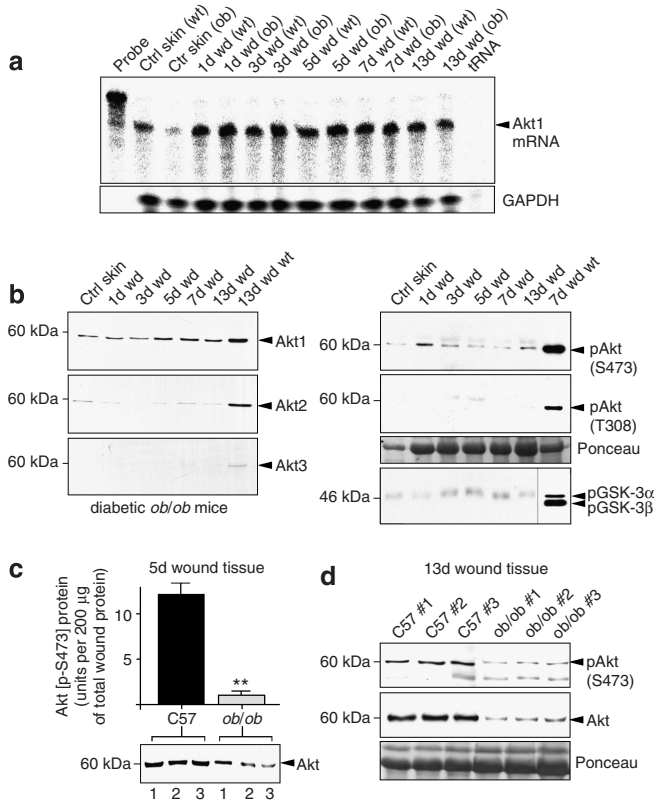

Figure 2. Expression and phosphorylation of Akt in diabetes-impaired skin repair. (**a**) RNase protection assay demonstrating Akt1 mRNA expression in nonwounded (ctrl skin) and wounded (wd) skin of healthy (wt) and diabetic *ob/ob* (ob) mice. 1,000 c.p.m. of the hybridization probe were added to the lane-labeled probe. Hybridization against GAPDH was used as a loading control. Every single data point depicts the mRNA isolated from four wounds ($n=4$). (**b**) Regulation of Akt protein expression (left panels) or phosphorylation (right panels) in diabetic *ob/ob* mice. The time after injury is indicated at the top of each lane. Ctrl skin refers to back skin biopsies of nonwounded mice. At 7- and 13-day (d) wd lysates from C57BL/6J mice (7-day wd wt, 13-day wd wt) were used to allow a direct comparison of pAkt expression levels. For immunoblot analysis, each time point depicts eight wounds ($n=8$) from four individual mice ($n=4$). One representative blot from three independent experimental animal series is shown. Loading of immunoblots was controlled using Ponceau S staining. (**c**) ELISA analyses from lysates of 5-day wd tissue isolated from wt (C57) and diabetic *ob/ob* mice. Phosphorylated (Ser473) Akt protein is expressed as units per 200 µg of total wd protein. **, $P<0.01$ (unpaired Student's *t*-test) as compared to control mice (C57). Bars indicate the mean ± SD obtained from wd lysates from four individual mice ($n=4$). The presence of total Akt protein from lysates of 5-day wd tissue from wt (C57) and diabetic *ob/ob* mice was analyzed below (1–3 = individual animals). (**d**) Immunoblot demonstrating the presence of phosphorylated and total Akt protein in 13-day wd lysates from healthy (C57) and diabetic (*ob/ob*) mice as indicated. Every single data point depicts two wounds from an individual animal. Loading of immunoblots was controlled using a Ponceau S staining.

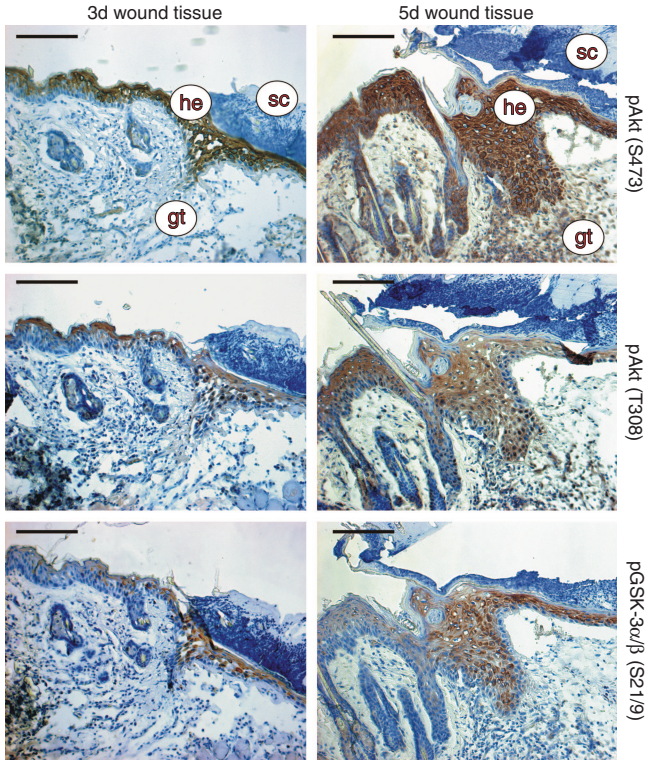

Figure 3. Localization of Akt in regenerating skin. Frozen serial sections from mouse wounds (days 3 and 5 (d) post-wounding) were incubated with polyclonal rabbit antisera directed against phosphorylated Akt (Ser473 or Thr308) or GSK-3α/β (Ser21/9) as indicated. All sections were stained with the avidin–biotin–peroxidase complex system using 3,3-diaminobenzidine-tetrahydrochloride as a chromogenic substrate. Nuclei were counterstained with hematoxylin. gt, granulation tissue; he, hyperproliferative epithelium, sc, scab. Bars, 50 µm.

appearance of phosphorylated Akt protein in wound margin keratinocytes was supported by an induction of Akt1- and Akt2-specific mRNA species at the wound margins. Although Akt1-3-specific mRNAs were constitutively expressed in the dermis of nonwounded skin, isolation of wound margin tissue from day 5 post-wounding (which contained the enriched keratinocyte fraction of the developing wound margin epithelia) revealed particularly strong signals for Akt1 and, to a lesser extent, for Akt-2 mRNA (Figure 4b), suggesting an induction of Akt1 mRNA expression in wound keratinocytes.

Although the S473 and T308 phospho-specific antibodies that had been used for immunoblot and histologic analyses have been generated against the Akt1 phospho-motifs, we could not absolutely differentiate for active Akt1 using these antibodies. Therefore, we now determined the predominant Akt isoform in skin and wound tissue as well as in cultured keratinocytes. To this end, we performed immunoprecipitation experiments using Akt1, -2, or -3-specific antisera. Results from the first set of experiments revealed Akt1 as the predominant isoform in normal and wounded skin tissue (Figure 4c). In addition, we performed immunoblots to detect the respective Akt protein isoforms directly from total cellular protein lysates of HaCaT. For this purpose, we separated two individual lanes each (IB no. 1, 2) of the filter after blotting and incubated the individual filter lanes with the respective anti-Akt1, -Akt2, or -Akt-3 antibodies as indicated. Incubation against a total Akt-specific antibody was used to control equal loading (lower panel). The filter sections were simultaneously exposed to the same film and exhibited

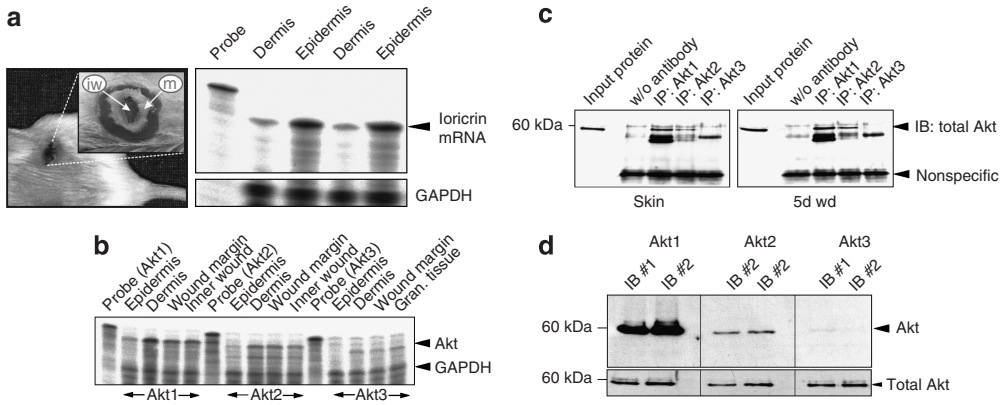

Figure 4. Isoform expression of Akt in regenerating skin. (**a**) Overview to show tissue sampling for inner wound and wound margin compartments (left panel). RNase protection assay demonstrating the distribution of epithelial-derived loricrin mRNA to control for separation of epidermis and dermis in tail skin tissue. Hybridization probe (1,000 c.p.m.) were added to the lane-labeled probe. Hybridization against GAPDH was used as a loading control. (**b**) RNase protection assay demonstrating distribution in expression of Akt1, Akt2, and Akt3 mRNA in epidermis and dermis of nonwounded skin or at the wound margin and inner wound (granulation tissue) on day 5 after injury as indicated. Every single data point depicts material isolated from four individual mice ($n=4$). Hybridization against GAPDH was used as a loading control. (**c**) Total protein (100 μg) from nonwounded skin (skin) or 5 day wounds were immunoprecipitated using Akt1-, Akt2, and Akt3-specific antibodies. Immunoprecipitates were analyzed by immunoblot and a total-Akt-specific antibody. Wound lysates were obtained from eight wounds ($n=8$) isolated from four individual mice ($n=4$) that have been pooled before analysis. (**d**) Total cellular protein (50 μg) from unstimulated HaCaT was analyzed for the presence of Akt1, Akt2, and Akt3 by immunoblot using Akt1-, Akt2-, or Akt3-specific antibodies as indicated. Staining of total Akt served as a loading control.

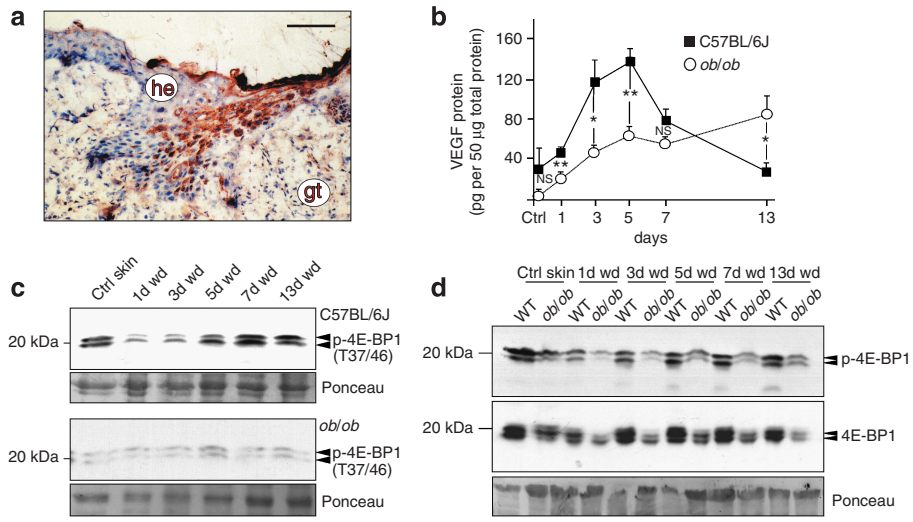

Figure 5. Reduced VEGF levels and 4E-BP1 phosphorylation in diabetes-impaired wound tissue. (**a**) Frozen sections from a mouse 5-day wound were incubated with a polyclonal rabbit antiserum directed against murine VEGF. Sections were stained with the avidin–biotin–peroxidase complex system using 3,3-diaminobenzidine-tetrahydrochloride as a chromogenic substrate. Nuclei were counterstained with hematoxylin. gt, granulation tissue; he, hyperproliferative epithelium. Bar, 25 μm. (**b**) VEGF ELISA analyses from lysates of nonwounded skin (ctrl) and lysates of wound tissue isolated from wild-type (C57BL/6J) and diabetic *ob/ob* mice. VEGF protein is expressed as pg per 50 μg skin or wound lysate. **, $P < 0.01$; *, $P<0.05$; NS, not significant (unpaired Student's *t*-test). Bars indicate the mean ± SD obtained from wound lysates from 12 individual mice ($n=12$). (**c**, **d**) Total protein (50 μg) from lysates of nonwounded skin (ctrl skin) and wound tissue (days 1, 3, 5, 7, and 13 after injury as indicated) isolated from wild-type (C57BL/6J) and *ob/ob* mice was analyzed by immunoblot for the presence of phosphorylated 4E-BP1 (p-4E-BP1). Expression of total 4E-BP1 was determined in (**d**, lower panel). Loading of immunoblots was controlled using a Ponceau S staining.

Akt1 as the major Akt isoform also in cultured human HaCaT (Figure 4d). Here it is important to note that transfection of HaCaT with an Akt1-specific small-interfering RNA (siRNA) again clearly confirmed the predominance of Akt1 protein in the cells. The completely abrogated signal for Akt1 upon Akt1 siRNA treatment of the cells was paralleled by a weak persisting signal in the total Akt control blot in lysates from siRNA-treated cells, unequivocally indicating the low expression level of Akt2 protein in HaCaT and also specificity of the Akt1 siRNA knockdown approach (Figure 8a).

Insulin-mediated VEGF synthesis in keratinocytes is controlled by a PI3K/Akt-dependent posttranscriptional regulatory mechanism. Wound margin keratinocytes are a major source of wound-derived VEGF (Brown *et al.*, 1992;

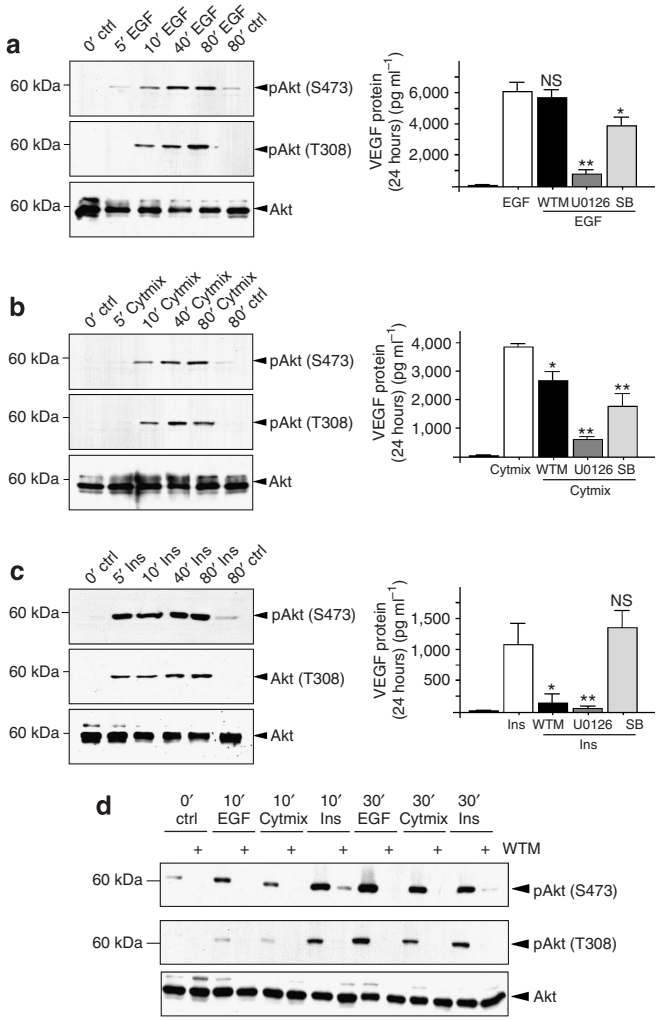

Figure 6. EGF-, cytokine-, and insulin-mediated Akt activation and VEGF production in cultured keratinocytes. Total cellular protein or cell culture supernatants from EGF- (**a**), cytokine (IL-1β, TNF-α, IFN-γ) (**b**), and insulin- (**c**) stimulated HaCaT were analyzed for either presence of Thr308- and Ser473-phosphorylated Akt protein at the indicated time points by immunoblot (upper panels) or for VEGF protein release by ELISA after 24 hours of stimulation in the presence or absence of the indicated protein kinase inhibitors (WTM, wortmannin; U0126; SB203580) (lower panels). Loading of immunoblot was controlled by analysis of total Akt protein. VEGF protein is expressed as pg per ml supernatant. **, $P<0.01$; *, $P<0.05$; NS, not significant (unpaired Student's *t*-test) as compared to stimulated (EGF, cytomix, insulin) conditions. Bars indicate the mean ± SD obtained from supernatants from three independent cell culture experiments ($n=3$). (**d**) Immunoblot for Thr308- and Ser473-phosphorylated Akt protein from EGF-, cytokine (IL-1β, TNF-α, IFN-γ) and insulin-stimulated HaCaT to control the inhibitory effect of wortmannin (WTM) on Akt phosphorylation.

Figure 5a) that was colocalized with activated Akt1 (Figure 3, see also Figure 11c, right panels) and markedly reduced in acute wounds of diabetic *ob/ob* mice during the acute phase of repair (Figure 5b, see also Figure 11b). The eucaryotic initiation factor 4E-BP1 represents a prominent target of the PI3K/Akt/mTOR pathway and has been shown to control VEGF production from keratinocytes (Gingras *et al.*, 2001; Segrelles *et al.*, 2004). Here we observed a clear loss of phosphorylated 4E-BP1 under conditions of diabetes-disturbed healing and reduced VEGF biosynthesis (Figure 5b–d). Comparable to conditions of Akt expression and phosphorylation in wound tissue (Figures 1 and 2), phosphorylated 4E-BP1 again reflected wound expression levels of total 4E-BP1 in normal and impaired wounds (Figure 5d).

Next, we investigated a functional connection between phosphorylated Akt and 4E-BP1 in the control of VEGF biosynthesis by wound-derived mediators in cultured keratinocytes. For this purpose, we stimulated quiescent cultured human HaCaT with epidermal growth factor (EGF), a combination of cytokines (IL-1β, tumor necrosis factor-α, IFN-γ) or insulin. As shown in Figure 6a–c, all applied stimuli mediated a rapid and robust phosphorylation of Akt in the cells (left panels), followed by large amounts of secreted VEGF protein (right panels). The inhibitor U0126 revealed a prominent role for p42/44 MAPK in EGF-, cytokine-, and insulin-mediated VEGF production, whereas effects of SB203580-inhibited p38 MAPK on VEGF synthesis were only moderate (for EGF and cytokines) or even absent (for insulin; Figure 6a–c, right panels).

Wortmannin potently inhibited EGF-, cytokine-, and insulin-stimulated Akt phosphorylation in the cells (Figure 6d), but it is important to note that inhibition of the PI3K/Akt pathway restrictively suppressed only insulin-stimulated VEGF expression from keratinocytes (Figure 6a–c, right panels). An overview over EGF-, cytokine-, and insulin-mediated VEGF mRNA expression in the presence or absence of U0126 or SB203580 (mRNA data to Figure 6a–c) is given in Figure S2. By contrast to EGF and cytokine treatments, insulin did not increase VEGF mRNA in the presence or absence of wortmannin (Figure 7a), suggesting a posttranscriptional mechanism of insulin action. In accordance, only insulin-mediated phosphorylation of 4E-BP1 became reduced upon wortmannin after 4 and 8 hours, but notably remained unaffected in EGF- and cytokine-stimulated keratinocytes (Figure 7b) at these time points. Phosphorylation of 4E-BP1 at the control time point (0′), which reflected quiescent keratinocytes pretreated by wortmannin for 30 minutes before the addition of stimuli, suggested that the observed constitutive phosphorylation of 4E-BP1 was dependent on a basal PI3K activity. In line with published data, rapamycin, added to interfere with 4E-BP1 phosphorylation downstream of Akt1, blunted 4E-BP1 phosphorylation, and subsequent production of VEGF in insulin-treated keratinocytes (Figure 7c). We did not consider p70S6 kinase for an additional analysis, as phosphorylation of p70S6 kinase has been shown to be not impaired in Akt1/2 double-knockout mice (Peng *et al.*, 2003).

Specific abrogation of Akt1 protein by siRNA completely abolishes insulin-induced VEGF biosynthesis in keratinocytes

Inhibition of the PI3K/Akt signaling pathway by wortmannin had shown a dramatic reduction in insulin-induced VEGF production from HaCaT (Figure 6c). To unequivocally prove the functional contribution of the Akt1 isoform in this process, we depleted functional Akt1 protein from the cells using an Akt1-specific siRNA approach. As shown in

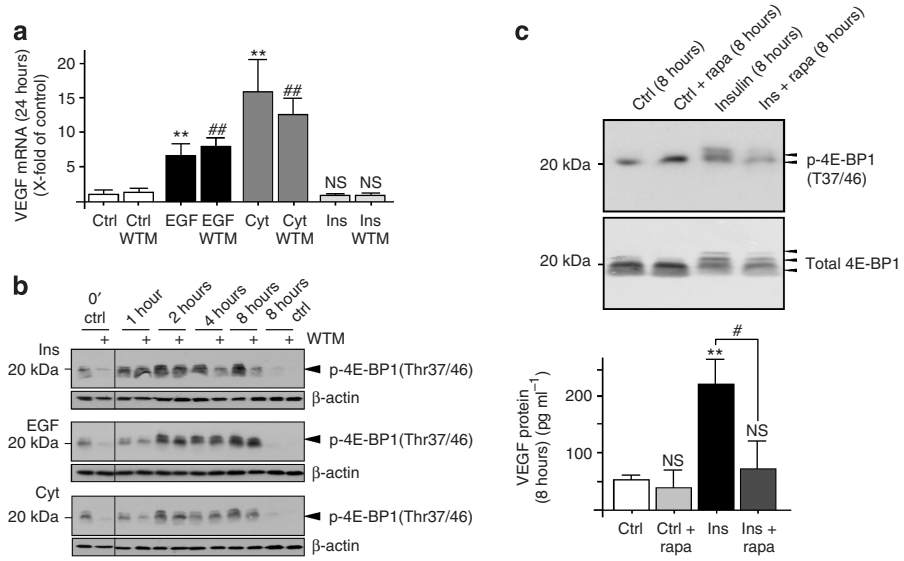

Figure 7. Insulin mediates VEGF expression by a posttranscriptional mechanism. (**a**) Quantification of VEGF mRNA (10-fold of control) after 24 hours of EGF, cytokine (IL-1β, TNF-α, IFN-γ) or insulin treatment in the presence or absence of wortmannin (WTM). **, $P<0.01$ as compared to nonstimulated ctrl; ##, $P<0.01$ as compared to WTM-treated ctrl; NS, not significant (unpaired Student's *t*-test) as compared to both controls. Bars indicate the mean ± SD obtained from three independent cell culture experiments ($n=3$). (**b**) Immunoblots of total cellular protein from insulin-, EGF-, or cytokine (ILL-1β, TNF-α, IFN-γ)-treated HaCaT were analyzed for phosphorylated 4E-BP1 (Thr37/46) in the presence or absence of wortmannin (WTM) at the indicated time points. β-Actin was used as a loading control. (**c**) Immunoblots of total cellular protein (50 μg) from insulin-treated HaCaT were analyzed for phosphorylated 4E-BP1 in the presence or absence of rapamycin (upper panel) after 8 hours of stimulation. One representative immunoblot out of three independent experiments is shown. Total 4E-BP1 was used as loading control. Respective supernatants from insulin-stimulated HaCaT were analyzed for VEGF protein release by ELISA after 8 hours of stimulation in the presence or absence of rapamycin (lower panel). VEGF protein is expressed as pg per ml supernatant. **, $P<0.01$; NS, not significant (unpaired Student's *t*-test) as compared to nonstimulated cells (ctrl). #, $P< 0.05$ as indicated by the bracket. Bars indicate the mean ± SD obtained from supernatants from three independent cell culture experiments ($n=3$).

Figure 8a (upper panel), Akt1 siRNA transfection potently abrogated Akt1 protein from keratinocytes. Moreover, the nearly complete loss of the total Akt protein signal (lower panel) upon Akt1 siRNA treatment clearly revealed Akt1 as the dominant Akt isoform in the cells. Importantly, the remaining weak signal for total Akt in parallel to the Akt1 siRNA knockdown again reflects not only the low expression level of Akt2 in keratinocytes (Figure 4d), but also Akt1 siRNA specificity, which is confirmed in addition by analysis of lysates using an Akt2-specific antibody (middle panel). As shown in Figure 4d, Akt 3 was not expressed and thus could not be assessed for expression in this particular experiment. In accordance to the inhibitor studies, we observed a complete dependence of insulin-induced VEGF protein biosynthesis on the presence of a functional Akt1 protein in keratinocytes (Figure 8b).

Constitutively active Akt1 confers an increase in keratinocyte VEGF production and drives phosphorylation of 4E-BP1 via activation of mTOR

To further scrutinize a regulatory role of activated Akt1 in keratinocyte VEGF production, we generated a myristoylated and thus constitutively active Akt1-Flag protein (Andjelkovic *et al.*, 1997; myrAkt1). Wild-type Akt1-Flag and an inactive Akt1-Flag mutant protein in which we had replaced Thr308 and Ser473 residues by Ala (Akt1-TASA) served as controls. Restricted localization of myrAkt1, but not of wild-type Akt1 and Akt1-TASA, at the plasma membrane suggested an active myrAkt1 in transfected cells (Figure 9a, lower panels). As HaCaT were hard to transfect, we controlled transfection efficiencies for the respective mutant proteins to enable correct determination of VEGF production (Figure 9a, upper panels and Figure 9b). Although myrAkt1 exhibited lowest transfection efficiencies, low numbers of myrAkt1-expressing cells remarkably represented the only conditions of significantly elevated levels of VEGF ($58 \pm 8\,pg\,ml^{-1}$) in transfected wells compared to background production from mock-treated cells (Figure 9c). Notably, calculated levels of VEGF assuming a transfection efficiency of 100% ($3052 \pm 421\,pg\,ml^{-1}$) were in the range of EGF- ($6032 \pm 682\,pg\,ml^{-1}$) and cytokine- ($3757 \pm 205\,pg\,ml^{-1}$) stimulated keratinocytes that had been used as positive controls in this set of experiments. In accordance, immunoprecipitation of wild-type and mutated Flag-tagged Akt1 revealed that only the VEGF-inducing myrAkt1 protein was phosphorylated at both Ser473 and Thr308 residues (Figure 9c, lower panel).

Immunofluorescence stainings for myrAkt1 and phosphorylated 4E-BP1 in the same set of keratinocyte transfection experiments clearly demonstrated 4E-BP1 phosphorylation in the presence of myrAkt1 (Figure 10, upper panel). To control the specificity of our immunofluorescence data, we added the mTOR inhibitor rapamycin to inhibit the PI3K/Akt/mTOR pathway downstream of Akt1 with respect to 4E-BP1 phosphorylation (Figure 10, middle

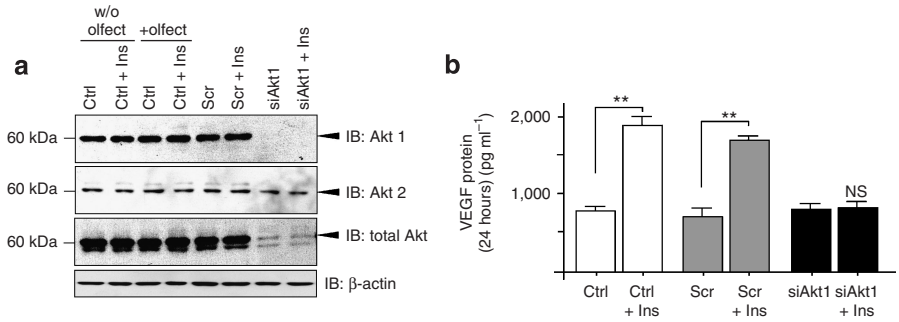

Figure 8. Specific abrogation of Akt1 by siRNA inhibits insulin-induced VEGF synthesis in keratinocytes. (**a**) Immunoblots demonstrating the efficiency of Akt1 depletion in HaCaT by specific siRNA transfection. Cells were left without (w/o olfect) or with (+olfect) transfection reagent oligofectamine in the presence or absence of insulin or treated with a scrambled (scr) or Akt1-specific (siAkt1) siRNA in the presence or absence of insulin. Akt1 depletion was controlled using a specific Akt1 (IB:Akt1), a specific Akt2 (IB:Akt2), or a total Akt (IB: total Akt) recognizing antibody. Loading of the immunoblot was controlled using β-actin. (**b**) Cell culture supernatants of the respective nontransfected (ctrl), scr- and siAkt1 siRNA-treated HaCaT shown in (**a**) were analyzed for VEGF protein release by ELISA after 24 hours of stimulation in the presence or absence of insulin. VEGF protein is expressed as pg per ml supernatant. **, $P<0.01$; NS, not significant (unpaired Student's *t*-test) as compared to nonstimulated conditions. Bars indicate the mean ± SD obtained from supernatants from three independent cell culture experiments ($n=3$).

panel). Transfection of inactive Akt1-TASA again demonstrated the specificity of the observed 4E-BP1 phosphorylation (Figure 10, lower panel).

Readjustment of insulin sensitivity in *ob/ob* mice restrictively mediates Akt1 phosphorylation and VEGF expression in wound margin keratinocytes. Finally, we used a leptin treatment of *ob/ob* mice to investigate whether the observed *in vitro* changes in Akt1 phosphorylation and VEGF expression were also dependent on insulin sensitivity *in vivo*. Therefore, mice were injected with recombinant leptin during skin repair. Leptin treatment is well established to resolve the obese and diabetic phenotype in *ob/ob* mice (Frank *et al.*, 2000; Goren *et al.*, 2006, 2007). We confirmed leptin effects in *ob/ob* mice by determination of blood glucose levels (Figure 11a), serum insulin, and body weight (Figure S3) in our animal experiment. Moreover, leptin treatment has been shown to readjust the strongly disturbed signaling from the insulin receptor in wound tissue of *ob/ob* mice and to improve wound healing (Frank *et al.*, 2000; Goren *et al.*, 2006).

Here we show that leptin-mediated resolution of insulin resistance in *ob/ob* mice was paralleled by a significant increase of the reduced wound VEGF protein observed in acute 5-day wounds of diabetic animals (Figure 11b). More important, only leptin treatment of *ob/ob* mice mediated a strong colocalization of phosphorylated Akt1 (red color) and VEGF protein (brown color) in wound keratinocytes of acute wounds (day 5 post-wounding; Figure 11c, right panels). By contrast, 5-day wound tissue of mock-treated *ob/ob* mice was characterized by the absence of abundant immunopositive signals for both phosphorylated Akt1 and VEGF (Figure 11c, left panels). These findings again argue for a functional connection of insulin sensitivity, Akt1 activation, and VEGF protein expression in wound keratinocytes.

Moreover, we observed a partial reappearance of Akt phosphorylation also in 13-day late wound tissue of leptin-treated *ob/ob* mice (Figure 11d). By contrast to conditions of acute healing at day 5 post-injury (Figure 11b), we observed highest levels of VEGF protein in chronic wound tissue of mock-treated *ob/ob* mice (Figure 11e). Double staining of wound tissues for phosphorylated Akt1 (red color) and VEGF (brown color) again exhibited that wound keratinocytes of the neoepidermis were responsible for the observed increase in Akt phosphorylation (red) and the only low level production of VEGF (brown) upon leptin treatment (Figure 11f, upper right panel), as granulation tissues of those wounds showed a complete absence of immunopositive signals for both proteins (Figure 11f, lower right panel). Here it is noteworthy that the weak signals for phosphorylated Akt in impaired wounds of mock-treated *ob/ob* mice (Figure 11d), resulted from a nearly complete absence of keratinocytes-expressing phosphorylated Akt in atrophied neoepidermal structures that failed to express high amounts of VEGF (Figure 11f, upper left panel; Figure 11e). More important, the increased VEGF protein levels in impaired 13-day wounds were produced from infiltrating immune cells, most likely macrophages, in an Akt-independent manner, as VEGF-positive cells in the granulation tissue (Figure 11f, lower left panel, brown) did not show any Akt1 phosphorylation (red).

DISCUSSION

At present there is growing evidence emphasizing a central role of Akt in skin biology, evidencing roles of Akt in keratinocyte biology. Activation of the PI3K/Akt signaling pathway controls cell survival in differentiating keratinocytes (Calautti *et al.*, 2005; Pankow *et al.*, 2006; Trash *et al.*, 2006). In addition, Akt1/Akt2 double-knockout mice displayed a translucent skin with thinner individual skin layers as compared to normal mice that could be attributed to a reduced proliferation of the basal keratinocytes (Peng *et al.*, 2003). In agreement with the known role of Akt in keratinocyte biology (Peng *et al.*, 2003; Calautti *et al.*, 2005; Pankow *et al.*, 2006; Trash *et al.*, 2006), we determined wound margin keratinocytes as the cellular source of activated Akt also during skin repair. Peng *et al.* (2003) noted Akt1 as the predominant Akt isoform in skin

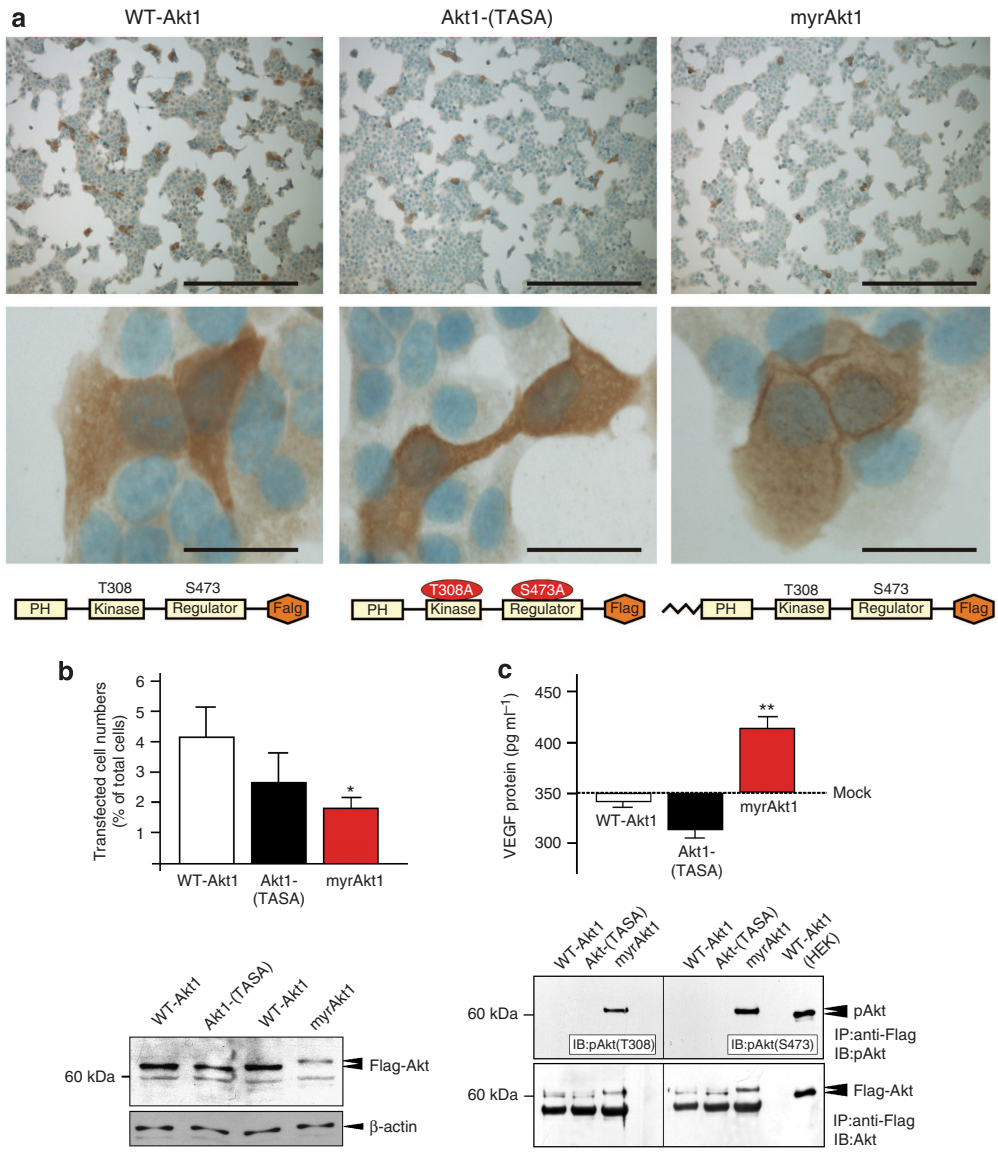

Figure 9. Constitutively active Akt1 mediates VEGF release from keratinocytes. HaCaT were transiently transfected with wild-type Akt1-Flag (WT-Akt1) and mutated Akt1-Flag constructs (Thr308 and Ser473 to Ala: TASA; myristoylated: myrAkt1) as indicated. (**a**) Transfection efficiencies for indicated Akt1-Flag proteins (upper panel). Transfected cells were immunostained using an anti-Flag antibody. A higher magnification showing cellular distribution of overexpressed Akt1-Flag proteins is shown in the lower panel. Bars, 180 μm (upper panels); 30 μm (lower panels). (**b**) Quantification of Akt1-Flag-transfected cell numbers (% of total cells) as indicated. *, $P<0.05$ (unpaired Student's *t*-test) as compared to WT-Akt1. Bars indicate the mean ± SD obtained from three independent cell culture experiments ($n=3$). The immunoblot shows an analysis of Flag-tagged Akt proteins from total protein lysates of transfected cells. Loading of the immunoblot was controlled using β-actin. (**c**, upper panel) Cell culture supernatants from transfected HaCaT were analyzed for VEGF protein by ELISA after 24 hours. VEGF protein is expressed as pg per ml supernatant. Transfection of the empty pCMV-Flag N3 plasmid served to determine VEGF background production from the cells (mock). **, $P<0.01$ (unpaired Student's *t*-test) as compared to mock-treated conditions. Bars indicate the mean ± SD obtained from supernatants from three independent cell culture experiments ($n=3$). (**c**, lower panel) recombinant Akt1 proteins were precipitated from lysates of transfected keratinocytes (WT-Akt1, Thr308, and Ser473 to Ala: TASA; myristoylated: myrAkt1) using anti-Flag agarose. Precipitates were subsequently analyzed for phosphorylated Thr308 and Ser473 residues by immunoblot. Equal loading was controlled using an anti-Flag antibody. WT-Akt1-transfected HEK cells served as a positive control.

tissue, and our experiments also demonstrated the Akt1 as the predominant isoform in wound tissue and cultured HaCaT. These observations were supported by data showing that proliferating human primary keratinocytes expressed only the Akt1 and 2 isoforms, from which only the targeted reduction of Akt1, but not 2, was functionally connected to the induction of keratinocyte cell death and the disruption of an organized expression of differentiation markers in organotypic skin cultures (Trash *et al.*, 2006). These *in vitro* findings, suggesting Akt1 to promote keratinocyte survival during differentiation, might find their *in vivo* counterparts during late skin repair. We observed activated Akt1 at mid- and late stages of acute repair (days 7 and 13 post-wounding), exactly when keratinocytes of the neoepithelial layer normally

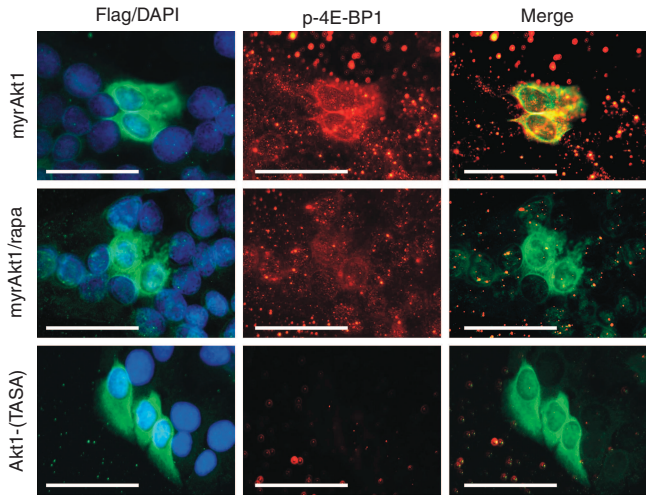

Figure 10. Constitutively active Akt1 stimulates phosphorylation of 4E-BP1 via activation of mTOR. HaCaT were transiently transfected with myristoylated Akt1-Flag (myrAkt1) in the absence (upper panel) or presence of rapamycin (middle panel) as indicated. myrAkt1(green) and phosphorylated 4E-BP1 (p-4E-BP1, red) proteins were subsequently analyzed by immunofluorescence. Transfection of cells with an inactive, mutated Akt1 (Thr308 and Ser473 to Ala: TASA) was performed as a negative control for 4E-BP1 phosphorylation (lower panel). Nuclei were stained with DAPI. Scale bar for all photographs = 10 μm.

cease to proliferate and start to structure the neoepithelium by subsequent differentiation (Martin, 1997; Singer and Clark, 1999). In good accordance, we found a marked increase in Akt1 phosphorylation restrictively originating in keratinocytes forming the robust neoepidermis following the leptin-mediated resolution of the insulin-resistant phenotype in *ob/ob* mice.

Along the same line, diabetes-impaired wound conditions in *ob/ob* mice revealed a loss of Akt1 activation during the complete period of repair. Diabetes-impaired wounds in *ob/ob* mice are characterized by severe defects in keratinocyte proliferation and thus cell numbers (Frank *et al.*, 2000). Moreover, we have recently reported a severe insulin resistance in wound tissue of *ob/ob* mice (Goren *et al.*, 2006), which was accompanied by an inhibition of insulin receptor downstream signaling and a loss of GSK-3α/β phosphorylation. Thus, data from this study close the gap, as we could now demonstrate also the absence of activated Akt1 in impaired wound tissue isolated from insulin-resistant *ob/ob* mice.

However, our study implicated additional roles of the PI3K/Akt signaling pathway in keratinocytes. Here we demonstrated that insulin, in addition to its functions as an endocrine hormone-type mediator, directly acts on VEGF gene expression during tissue regeneration. This observation strongly indicates that the described insulin resistance in wound tissue of diabetic *ob/ob* mice (Goren *et al.*, 2006) might not only interfere with resident glucose uptake and metabolism. In addition, insulin and insulin-like growth factor 1 have been shown to actively regulate VEGF expression in several *in vitro* and *in vivo* model systems such as cardiomyocytes, thyroid carcinoma cells, or retinal epithelial cells (Treins *et al.*, 2002; Jiang *et al.*, 2003; Poulaki *et al.*, 2003; He *et al.*, 2006). Notably, it was unique to insulin here that VEGF production from keratinocytes could be completely blocked by interference with PI3K/Akt signaling. Inhibition of PI3K/Akt resulted in a delayed reduction of 4E-BP1 phosphorylation and a subsequent inhibition of VEGF translation. The delayed appearance of dephosphorylated 4E-BP1 protein upon wortmannin-mediated inhibition of insulin action might result from early compensatory kinase activities, especially that of p42/44 MAPK, which essentially contributed to insulin-stimulated VEGF release from keratinocytes (this study). Thus, it is tempting to suggest a so far not appreciated contribution of insulin to wound-derived VEGF production in skin repair. This function might participate in decreased levels of wound-derived VEGF associated with wound healing disorders (Frank *et al.*, 1995; Lauer *et al.*, 2000; Kämpfer *et al.*, 2001; Stallmeyer *et al.*, 2001; Roth *et al.*, 2006; this study). The proposed previously unknown function of insulin in tissue repair is further supported by our observation that the resolution of insulin resistance in *ob/ob* mice by leptin translated into a wound margin keratinocyte-restricted reappearance of Akt1 phosphorylation and a stringently colocalized VEGF protein in the cells.

Thus, our data are in clear accordance to Akt1-overexpressing murine keratinocytes that displayed a tumorigenic VEGF-mediated angiogenic switch that was clearly attributed to an elevated translation of VEGF-specific mRNA and increased phosphorylation of 4E-BP1 (Segrelles *et al.*, 2004). As also expression of matrix metalloproteinase-2 and -9 was coinduced by the similar posttranscriptional mechanism (Segrelles *et al.*, 2004) and as Akt1 overexpression mediated an augmentation of also keratinocyte glucose uptake (I Goren, unpublished data), one might speculate that cellular consequences of insulin-driven Akt activation might not be restricted to wound VEGF production. Along this line of argumentation, two most recent papers connected epithelial Akt activation to the process of skin carcinogenesis. As mentioned above, Akt contributes to the tumor–stroma relationship by enhancing angiogenic processes (Segrelles *et al.*, 2004). In addition, PI3K and subsequent Akt activation have been described as early key events in chemically induced models of skin tumorigenesis in mice (Segrelles *et al.*, 2002). In accordance, keratinocyte-directed overexpression of Akt in transgenic mice mediated a generalized hyperplasia of the interfollicular epidermis and the hair follicles (Segrelles *et al.*, 2007). Here it is reasonable to argue that skin wounding appeared to initiate those functions of the Akt1 protein that are connected to keratinocyte proliferative and angiogenic responses to enable and drive a physiologic response toward tissue regeneration.

In summary, we have shown that Akt1 was the predominant Akt isoform in skin repair. Our data on posttranscriptional control of insulin-stimulated VEGF expression via Akt1 suggest a role of insulin in the control of keratinocyte angiogenic potential in wound healing. As a severe insulin resistance has been described in skin and wound tissue of diabetic mice (Goren *et al.*, 2006), which most probably also blunts Akt activation after wounding (this study), loss of Akt-mediated VEGF release from insulin-resistant wound margin

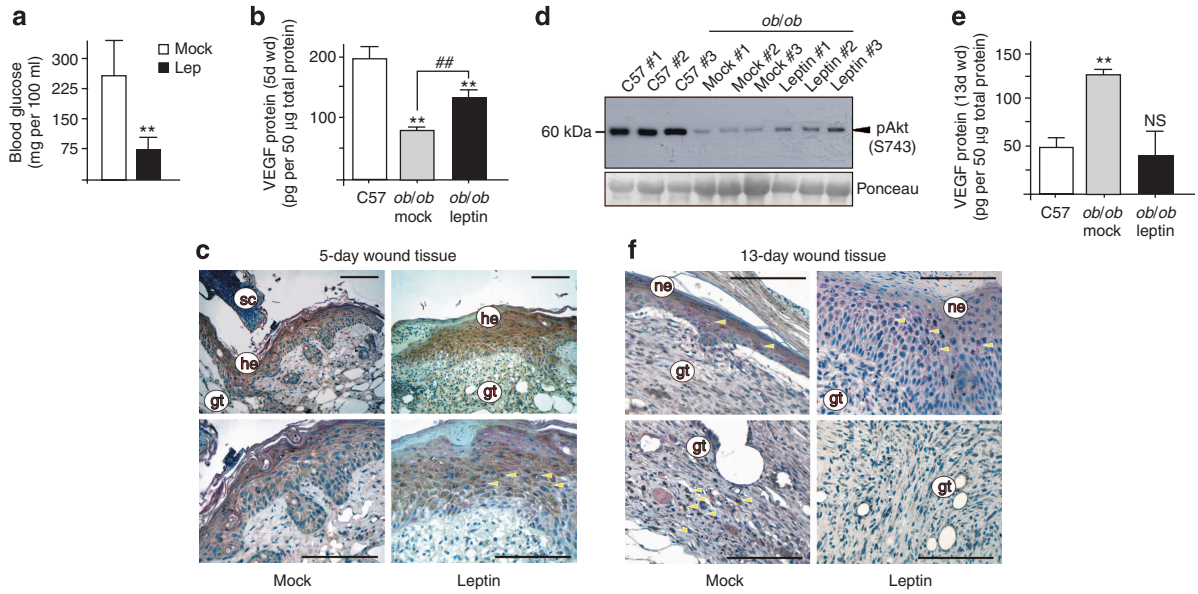

Figure 11. Activated Akt1 colocalizes with VEGF protein in wound keratinocytes upon improvement of insulin sensitivity in *ob/ob* mice. (**a**) Blood glucose levels in *ob/ob* mice 3 hours after systemic leptin administration. PBS-treated mice served as mock controls. (**b**) VEGF-specific ELISA analyses of 5-day wound tissue lysates from wild-type (C57), PBS-treated (*ob/ob* mock) or leptin-treated (*ob/ob* leptin) *ob/ob* mice. VEGF protein is expressed as pg per 50 µg wound lysate. **, $P<0.01$ (unpaired Student's *t*-test) as compared to C57 control animals. ##, $P<0.01$ as indicated by brackets. Bars indicate the mean ± SD obtained from wound lysates from four individual mice ($n=4$). (**c**) Frozen sections from PBS-treated (mock) and leptin-treated *ob/ob* mouse wounds (day 5 post-injury) were coincubated with antisera directed against murine phosphorylated Akt (Ser473) and murine VEGF. Sections were stained with the avidin–biotin–peroxidase complex system and different chromogenic substrates. Immunopositive signals for phosphorylated Akt (Ser473; red) and for VEGF (brown) visualize the coexpression of activated Akt and VEGF proteins in wound tissue. Particularly double-stained cells (red: Akt and brown: VEGF) were indicated by yellow arrows. Nuclei were counterstained with hematoxylin. gt, granulation tissue; he, hyperproliferative epithelium; sc, scab. Bar, 25 µm. (**d**) Immunoblot demonstrating the presence of phosphorylated Akt (Ser473) protein in 13 day wound lysates from healthy (C57), PBS-treated diabetic (mock) and leptin-treated (leptin) *ob/ob* mice. Every single data point depicts two wounds from an individual animal. Loading of the immunoblot was controlled using a Ponceau S staining. (**e**) VEGF-specific ELISA analyses of 13-day wound tissue lysates from wild-type (C57), PBS-treated (*ob/ob* mock) or leptin-treated (*ob/ob* leptin) *ob/ob* mice. VEGF protein is expressed as pg per 50 µg-wound lysate. **, $P<0.01$; NS, not significant (unpaired Student's *t*-test) as compared to C57 control animals. Bars indicate the mean ± SD obtained from wound lysates from four individual mice ($n=4$). (**f**) Frozen sections from PBS-treated (mock) and leptin-treated *ob/ob* mouse wounds (day 13 post-injury) were coincubated with antisera directed against murine phosphorylated Akt (Ser473) and murine VEGF. Sections were stained with the avidin–biotin–peroxidase complex system and different chromogenic substrates. Immunopositive signals for phosphorylated Akt (Ser473, red) and for VEGF (brown) visualize the coexpression of activated Akt and VEGF proteins in wound tissue. Particularly double-stained cells (red: Akt and brown: VEGF) were indicated by yellow arrows. Nuclei were counterstained with hematoxylin. gt, granulation tissue; ne, neoepidermis. Bar, 25 µm.

keratinocytes might further aggravate the problem of reduced angiogenesis in diabetes-impaired wounds.

MATERIALS AND METHODS

Animals

Female C57BL/6J (wild-type) and C57BL/6J-*ob/ob* mice (*Mus musculus*) were obtained from Charles River (Sulzfeld, Germany). At the age of 10 weeks, mice were caged individually, monitored for body weight, and wounded as described below.

Treatment of mice

Murine recombinant leptin (Calbiochem, Bad Soden, Germany) was injected intraperitoneally (2 µg g^{-1} body weight, one injection per day, from 2 days before wounding until day 13 post-wounding). A daily injection of phosphate-buffered saline (mock) was used as a control.

Wounding of mice

Wounding of mice was performed as described previously (Frank *et al.*, 1999; Stallmeyer *et al.*, 1999). Briefly, six full-thickness wounds (5 mm in diameter, 3–4 mm apart) were made on the back of each mouse by excising the skin and the underlying panniculus carnosus. Skin biopsy specimens were obtained from the animals 1, 3, 5, 7, and 13 days after injury. Nonwounded back skin served as a control. Wounds ($n=48$) isolated from animals ($n=12$) from three independent animal experiments were used for RNA analysis. For immunoblot analysis, wounds ($n=8$) from four individual mice ($n=4$) were used. All animal experiments were performed according to the guidelines and approval of the local Ethics Animal Review Board.

Determination of blood glucose, insulin, and leptin levels

Blood glucose levels were determined using the Accutrend sensor (Roche Biochemicals, Mannheim, Germany). Serum insulin and leptin were analyzed by enzyme-linked immunosorbent assay (Crystal Chemicals, Chicago, IL) as described by the manufacturer.

Cell culture

Quiescent human HaCaT (Boukamp *et al.*, 1988) were stimulated with EGF (10 ng ml^{-1}), insulin (2 µg ml^{-1}), or with a combination of

cytokines (2 nM IL-1β, 2 nM tumor necrosis factor-α, 100 U ml^{-1} interferon (IFN)-γ) in the presence or absence of 200 nM wortmannin, 10 μM U0126, 5 μM SB203580, or 50 ng ml^{-1} rapamycin for the indicated periods of time. EGF, IFN-γ, and insulin were purchased from Roche Biochemicals and IL-1βor tumor necrosis factor-α was from Peprotec (Hanau, Germany). Wortmannin and SB203580 were obtained from Calbiochem (Darmstadt, Germany) and U0126 was from Alexis (San Diego, USA). Rapamycin (50 ng ml^{-1}) was also used in the transfection studies and obtained from Calbiochem (Darmstadt, Germany).

Silencing of Akt1 expression by siRNA

HaCaT (2×10^5) were grown in six-well plates to reach 40–60% confluency. Cells were subsequently transfected twice with siRNA (50 nM final concentration) using oligofectamine (Invitrogen, Karlsruhe, Germany) and OptiMEM (Invitrogen) as described by the manufacturer. The Akt1-specific siRNA was purchased from Applied Biosystems (Darmstadt, Germany).

RNA isolation and RNase protection analysis

RNA isolation and RNase protection assays were carried out as described previously (Chomczynski and Sacchi, 1987; Frank *et al.*, 1999). The murine cDNA corresponded to nucleotides 1598–1917 (for Akt1, X65687), 1437–1701 (for Akt2, U22445), 1451–1710 (for Akt3, AF124142), 139–585 (for VEGF, S38083), 3998–4183 (for loricrin, U09189.1), or 163–317 (for GAPDH, NM002046) of the published sequences. The human cDNA corresponded to 339–498 (for VEGF, (Weindel *et al.*, 1992) or 961–1070 (for GAPDH, M33197) of the published sequences. Total cellular RNA from keratinocytes of three independent cell culture experiments ($n = 3$) was analyzed by RNase protection assay.

Preparation of protein lysates and immunoblot analysis

Murine skin and HaCaT culture samples were homogenized as described (Kämpfer *et al.*, 1999; Goren *et al.*, 2006). Cytoplasmic and nuclear fractions were generated according to a published protocol (Schreiber *et al.*, 1989). Protein concentrations were determined using the BCA Protein Assay Kit (Pierce Inc., Rockford, IL, USA). Total protein lysate (20–50 μg) was separated using SDS-gel electrophoresis, and specific proteins were detected using antisera directed against Akt1 (Biomol, Hamburg, Germany and Epitomics, Hamburg, Germany), total Akt or Akt2, Akt3, phosphorylated Akt (Ser473), phosphorylated Akt (Thr308), phospho-GSK-3α/β (Ser21/9), phospho-eucaryotic initiation factor 4E-BP1 (Thr37/46), total 4E-BP1 (Cell Signaling, New England Biolabs, Frankfurt, Germany), Flag fusion proteins (Sigma, Taufkirchen, Germany), nucleolin and insulin receptor-β (Santa Cruz, Heidelberg, Germany), respectively. A secondary antibody coupled to horseradish peroxidase and the ECL detection system was used to visualize the proteins of interest. Phenylmethylsulfonyl fluoride, aprotinin, NaF, Na_2VO_4, and dithiothreitol were from Sigma. Ocadaic acid and leupeptin were from BioTrend (Köln, Germany) and the ECL detection system was obtained from Amersham (Freiburg, Germany).

Separation of epidermis and dermis layer of mouse tail skin

Mouse tail skin was incubated for 30 minutes at 37 °C in a solution of 2 M NaBr. The epidermis was separated from the underlying dermis, immediately frozen in liquid nitrogen and used for subsequent analyses.

Immunoprecipitation

Total wound or cell culture lysate (200 μg) was incubated overnight with the respective Akt1- (Epitomics and Biomol), Akt2-, Akt3- (Cell Signaling), or Flag- (Sigma) specific antibodies according to instructions of the manufacturer. Immunoprecipitates were isolated using protein G sepharose (Sigma). Flag-tagged Akt1 was immunoprecipitated using an anti-Flag M2 affinity gel (Sigma) in 500 μl of Flag buffer (25 mM Tris-Cl, pH 7.4, 150 mM NaCl, 1 mM CaCl2, 1% Triton X-100). Protein G sepharose- and Flag-bound precipitates were washed in TBST (150 mM NaCl, 10 mM Tris-Cl, pH 8.0, 0,05% Tween 20) and protein was eluted using Laemmli buffer. Triton X-100 and Tween 20 were obtained from Sigma.

Enzyme-linked immunosorbent assay

Quantification of human or mouse VEGF protein was performed using the human or mouse VEGF Quantikine ELISA kit (R&D systems, Wiesbaden, Germany). Supernatants from three independent cell culture experiments ($n = 3$) were analyzed. Phosphorylated Akt (S473) protein was quantified in wound lysates using the Akt (pS473) immunoassay kit (Biosource, Nivelles, Belgium).

Immunohistochemistry

Mice were wounded as described above. Animals were killed at days 3 and 5 after injury. Complete wounds were isolated from the back, bisected, and frozen in tissue freezing medium. Frozen sections (6 μm) were subsequently analyzed using immunohistochemistry as described (Stallmeyer *et al.*, 1999). Antisera against phosphorylated Akt (Ser473), phosphorylated Akt (Thr308), phospho-GSK-3α/β (Ser21/9; Cell Signaling), or VEGF (Santa Cruz) were used for immunodetection.

Immunocytochemistry

HaCaT keratinocytes were grown on glass slides until they reached 50% confluency. Cells were fixed using methanol/EDTA (0.02% w/v) for 15 minutes at −20 °C. Immunostaining was performed using an anti-Flag antibody (1:200 dilution; Sigma) according to the ABC peroxidase staining kit from Santa Cruz.

Immunofluorescence

HaCaT keratinocytes were grown on glass slides and stimulated with insulin (2 μg ml^{-1}) as described above. Control and stimulated cells were subsequently fixed using methanol/EDTA (0.02% w/v) or paraformaldehyde (2% w/v) for 15 minutes at −20 °C or room temperature, respectively. Fixed cells were blocked with 5% goat serum diluted in phosphate-buffered saline/Triton (0.1% w/v). Antisera against Flag fusion proteins (Sigma) and phosphorylated 4E-BP1 (Thr37/46; Cell Signaling) were incubated for 1 hour at room temperature. The fluorescence-coupled secondary antibodies Alexa Fluor 488 (Molecular Probes, Leiden, The Netherlands) or Cy3 (Dianova, Hamburg, Germany) were diluted 1:250 in 5% goat serum/phosphate-buffered saline and incubated in the dark for 30 minutes. Nuclei were counterstained using 4′,6-diamidino-2-phenylindole (Sigma).

Generation of mutated and Akt1-Flag fusion constructs

A full-length human Akt1 cDNA was amplified from total HaCaT keratinocyte cDNA using plaque-forming unit polymerase (Promega, Mannheim, Germany) and 5′-GATAGAATTCGGGCACCATGAGC

GACG-3′ and 5′-CTATGGATCCGGCCGTGCTGCTGGC-3′ as primers. Amplicons were cloned into *Eco*RI/*Bam*HI sites of pCMV-Flag N3 (kindly provided by M Bachmann) (Bachmann *et al.*, 2004). The pCMV-NE-Akt1-Flag was used as a template for subsequent cloning strategies. Mutation of Akt1 Thr308 and Ser473 residues was performed using the pCMV-NE-Akt1-Flag vector as a template, the QuickChange Site-Directed Mutagenesis Kit (Stratagene, Heidelberg, Germany) and the following primers: 5′-GGTGCCACCAT GAAGGCCTTTTGCGGCACAC-3′ (for the Thr308 to Ala mutation, Akt1-T308A) and 5′-CCCACTTCCCCCAGTTCGCGTACTCGGCCA GCAGCACG-3′ (for the Ser473 to Ala mutation, Akt1-S473A). The Ser473 and Thr308 to Ala Akt1 double mutant was generated by cloning an *Eco*RI/*Hin*dIII fragment of pCMV-NE-Akt1-T308A into pCMV-NE-Akt1-S473A from which the *Eco*RI and *Hin*dIII was removed (pCMV-NE-Akt1-TASA). A myristoylated form of Akt1 was cloned by PCR using pCMV-NE-Akt1-Flag as template and 5′-AGATCTCGAGCCACCATGGGGAGTAGCAAGAGCAAGCCTAAG GACCCCAGCCAGCGCGCTAGCGACGTGGCTATTGTG-3′ (harboring the *v-src* myristoylation signal) and 5′-CCACATCCTGCGGCC-3′ as primers. Amplicons were digested with *Not*I and subcloned into the *Nhe*I/*Not*I site of pCMV-Akt1-Flag-N3 (myr-Akt1).

Transfection experiments

HEK293 and HaCaT cells were transiently transfected with FuGene transfection reagent (Roche Biochemicals) and the appropriate plasmid DNA according to the instructions of the manufacturer.

Statistical analysis

Data are shown as means ± SD. Data analysis was carried out using the unpaired Student's *t*-test with raw data. Statistical comparison between more than two groups was carried out by analysis of variance (Dunnett's method).

CONFLICT OF INTEREST

The authors state no conflict of interest.

ACKNOWLEDGMENTS

We thank Dr A Theisen for his help with the animal experiments and Dr Malte Bachmann for the pCMV-Flag N3 vector. This study was supported by the Deutsche Forschungsgemeinschaft (SFB 553, grant FR 1540/1-2, GK 1172, and Excellence Cluster Cardio-Pulmonary System), by Eicosanox, EC FP6 funding (LSHM-CT-2005-005033), and Nachlässe Held-Hecker.

SUPPLEMENTARY MATERIAL

Figure S1. Localization of Akt in regenerating skin.

Figure S2. VEGF mRNA expression in EGF-, cytokine-, and insulin-treated keratinocytes in the presence of U0126 and SB203580.

Figure S3. Systemic leptin treatment improves the insulin resistant and obese phenotype in *ob/ob* mice.

REFERENCES

Andjelkovic M, Alessi DR, Meier R, Fernandez A, Lamb NJ, Frech M *et al.* (1997) Role of translocation in the activation and function of protein kinase B. *J Biol Chem* 272:31515–24

Apelqvist J, Larsson J, Agardh CD (1993) Long-term prognosis for diabetic patients with foot ulcers. *J Intern Med* 233:485–91.

Bachmann M, Hennemann H, Xing PX, Hoffmann I, Möröy T (2004) The oncogenic serine/threonine kinase Pim-1 phosphorylates and inhibits the activity of Cdc25C-associated kinase 1 (C-TAK1). *J Biol Chem* 279:48319–28

Boukamp P, Petrussevsak RT, Breitkreuz D, Hornung J, Markham A, Fusenig N (1988) Normal keratinization in a spontaneously immortalized aneuploid human keratinocyte cell line. *J Cell Biol* 106:761–71

Boulton AJM (2004) The diabetic foot: from art to science. The 18th Camillo Golgi lecture. *Diabetologia* 47:1343–53

Brown LF, Yeo KT, Berse B, Yeo TK, Senger DR, Dvorak HF *et al.* (1992) Expression of vascular permeability factor (vascular endothelial growth factor) by epidermal keratinocytes during wound healing. *J Exp Med* 176:1375–9

Calautti E, Li J, Saoncella S, Brisette JL, Goetinck PF (2005) Phosphoinositide 3-kinase signaling to Akt promotes keratinocyte differentiation versus death. *J Biol Chem* 280:32856–65

Carrington AL, Abbott CA, Griffiths J, Jackson N, van Ross ERE, Boulton AJM (2001) A foot care program for diabetic unilateral amputees. *Diabetes Care* 24:216–21

Chomczynski P, Sacchi N (1987) Single-step method of RNA isolation by acid guanidinium thiocyanate-phenol-chloroform extraction. *Anal Biochem* 162:156–9

Cross DA, Alessi DR, Cohen P, Andjelkovich M, Hemmings BA (1995) Inhibition of glycogen synthase kinase-3 by insulin mediated by protein kinase B. *Nature* 378:785–9

Faglia E, Favales F, Morabito A (2001) New ulceration, new major amputation, and survival rates in diabetic subjects hospitalized for foot ulceration from 1990 to 1993: a 6.5 year follow-up. *Diabetes Care* 24:78–83

Frank S, Hübner G, Breier G, Longaker MT, Greenhalgh DG, Werner S (1995) Regulation of vascular endothelial growth factor expression in cultured keratinocytes. Implications for normal and impaired wound healing. *J Biol Chem* 270:12607–13

Frank S, Stallmeyer B, Kämpfer H, Kolb N, Pfeilschifter J (1999) Nitric oxide triggers enhanced induction of vascular endothelial growth factor expression in cultured keratinocytes (HaCaT) and during cutaneous wound repair. *FASEB J* 13:2002–14

Frank S, Stallmeyer B, Kämpfer H, Kolb N, Pfeilschifter J (2000) Leptin enhances wound re-epithelialization and constitutes a direct function of leptin in skin repair. *J Clin Invest* 106:501–9

Franke TF, Yang SI, Chan TO, Datta K, Kazlauskas A, Morrison DK *et al.* (1995) The protein kinase encoded by the Akt proto-oncogene is a target of the PDGF-activated phosphatidylinositol 3-kinase. *Cell* 81:727–37

Gingras AC, Raught B, Sonenberg N (2001) Regulation of translation initiation by FRAP/mTOR. *Genes Dev* 15:807–26

Goren I, Kämpfer H, Podda M, Pfeilschifter J, Frank S (2003) Leptin and wound inflammation in diabetic ob/ob mice: differential regulation of neutrophil and macrophage influx and a potential role for the scab as a sink for inflammatory cells and mediators. *Diabetes* 52: 2821–32

Goren I, Müller E, Pfeilschifter J, Frank S (2006) Severely impaired insulin signaling in chronic wounds of diabetic ob/ob mice. A potential role of tumor necrosis factor-α. *Am J Pathol* 168:765–77

Goren I, Müller E, Schiefelbein D, Christen U, Mühl H, Pfeilschifter J *et al.* (2007) Systemic anti-TNFalpha treatment restores diabetes-impaired skin repair in ob/ob mice by inactivation of macrophages. *J Invest Dermatol* 127:2259–67

He Z, Opland DM, Way KJ, Ueki K, Bodyak N, Kang PM *et al.* (2006) Regulation of vascular endothelial growth factor expression and vascularization in the myocardium by insulin receptor and PI3K/Akt pathways in insulin resistance and ischemia. *Arterioscler Thromb Vasc Biol* 26:787–93

Jiang ZY, He Z, King BL, Kuroki T, Opland DM, Suzuma K *et al.* (2003) Characterization of multiple signaling pathways of insulin in the regulation of vascular endothelial growth factor expression in vascular cells and angiogenesis. *J Biol Chem* 278:31964–71

Kämpfer H, Kalina U, Mühl H, Pfeilschifter J, Frank S (1999) Counter-regulation of interleukin-18 mRNA and protein expression during cutaneous wound repair. *J Invest Dermatol* 113:369–74

Kämpfer H, Pfeilschifter J, Frank S (2001) Expressional regulation of angiopoietin-1 and -2 and the Tie-1 and -2 receptor tyrosine kinases during cutaneous wound healing: a comparative study of normal and impaired repair. *Lab Invest* 81:361–73

Lauer G, Sollberg S, Cole M, Flamme I, Sturzebecher J, Mann K *et al.* (2000) Expression and proteolysis of VEGF is increased in chronic wounds. *J Invest Dermatol* 115:12–8

Loots MA, Lamme EN, Zeegelaar J, Mekkes JR, Bos JD, Middelkoop E (1998) Differences in cellular infiltrate and extracellular matrix of chronic diabetic and venous ulcers versus acute wounds. *J Invest Dermatol* 111:850–7

Martin P (1997) Wound healing—aiming for perfect tissue regeneration. *Science* 276:75–81

Pankow S, Bamberger C, Klippel A, Werner S (2006) Regulation of epidermal homeostasis and repair by phosphoinositide 3-kinase. *J Cell Sci* 119:4033–46

Peng XD, Xu PZ, Chen ML, Hahn-Windgassen A, Skeen J, Jacobs J *et al.* (2003) Dwarfism, impaired skin development, skeletal muscle atrophy, delayed bone development, and impeded adipogenesis in mice lacking Akt1 and Akt2. *Genes Dev* 17:1352–65

Plas DR, Thompson CB (2005) Akt-dependent transformation: there is more to growth than just surviving. *Oncogene* 24:7435–42

Poulaki V, Mitsiades CS, McMullan C, Sykoutri D, Fanourakis G, Kotoula V *et al.* (2003) Regulation of vascular endothelial growth factor expression by insulin-like growth factor I in thyroid carcinomas. *J Clin Endocrinol Metab* 88:5392–8

Reiber GE, Ledoux WR (2002) Epidemiology of diabetic foot ulcers and amputations: evidence for prevention. In: *The Evidence Base for Diabetes Care*. (Williams R, Herman W, Kinmoth AL, Wareham NJ (eds). Wiley: Chichester, UK, 641–65

Roth D, Piekarek M, Paulsson M, Christ H, Krieg T, Bloch W *et al.* (2006) Plasmin modulates vascular endothelial growth factor-A-mediated angiogenesis during wound repair. *Am J Pathol* 168:670–84

Sarbassov DD, Guertin DA, Ali SM, Sabatini DM (2005) Phosphorylation and regulation of Akt/PKB by the rictor-mTOR complex. *Science* 307:1098–101

Schreiber E, Matthias P, Müller MM, Schaffner W (1989) Rapid detection of octamer binding proteins with 'mini-extracts', prepared from a small number of cells. *Nucleic Acids Res* 17:6419

Segrelles C, Lu J, Hammann B, Santos M, Moral M, Cascallana JL *et al.* (2007) Deregulated activity of Akt in epithelial basal cells induces spontaneous tumors and heightened sensitivity to skin carcinogenesis. *Cancer Res* 67:10879–88

Segrelles C, Ruiz S, Perez P, Murga C, Santos M, Budunova IV *et al.* (2002) Functional roles of Akt signaling in mouse skin tumorigenesis. *Oncogene* 21:53–64

Segrelles C, Ruiz S, Santos M, Martinez-Palacio J, Lara MF, Paramio JM (2004) Akt mediates an angiogenic switch in transformed keratinocytes. *Carcinogenesis* 25:1137–47

Singer AJ, Clark RAF (1999) Cutaneous wound healing. *N Engl J Med* 341:728–46

Stallmeyer B, Kämpfer H, Kolb N, Pfeilschifter J, Frank S (1999) The function of nitric oxide in wound repair: inhibition of inducible nitric oxide synthase severely impairs wound reepithelialization. *J Invest Dermatol* 113:1090–8

Stallmeyer B, Pfeilschifter J, Frank S (2001) Systemically and topically supplemented leptin fails to reconstitute a normal angiogenic response during skin repair in diabetic ob/ob mice. *Diabetologia* 44: 471–9

Testa JR, Tsichlis PN (2005) Akt signaling in normal and malignant cells. *Oncogene* 24:7391–3

Trash BR, Menges CW, Pierce RH, McCance DJ (2006) Akt1 provides an essential survival signal required for differentiation and stratification of primary human keratinocytes. *J Biol Chem* 281: 12155–62

Treins C, Giorgetti-Peraldi S, Murdaca J, Semenza GL, Van Obberghen E (2002) Insulin stimulates hypoxia-inducible factor 1 through a phosphatidylinositol 3-kinase/target of rapamycin-dependent signaling pathway. *J Biol Chem* 277:27975–81

Weindel K, Marme D, Weich HA (1992) AIDS-associated Kaposi's sarcoma cells in culture express vascular endothelial growth factor. *Biochem Biophys Res Commun* 183:1167–74

Wetzler C, Kämpfer H, Stallmeyer B, Pfeilschifter J, Frank S (2000) Large and sustained induction of chemokines during impaired wound healing in the genetically diabetic mouse: prolonged persistence of neutrophils and macrophages during the late phase of repair. *J Invest Dermatol* 115:245–52